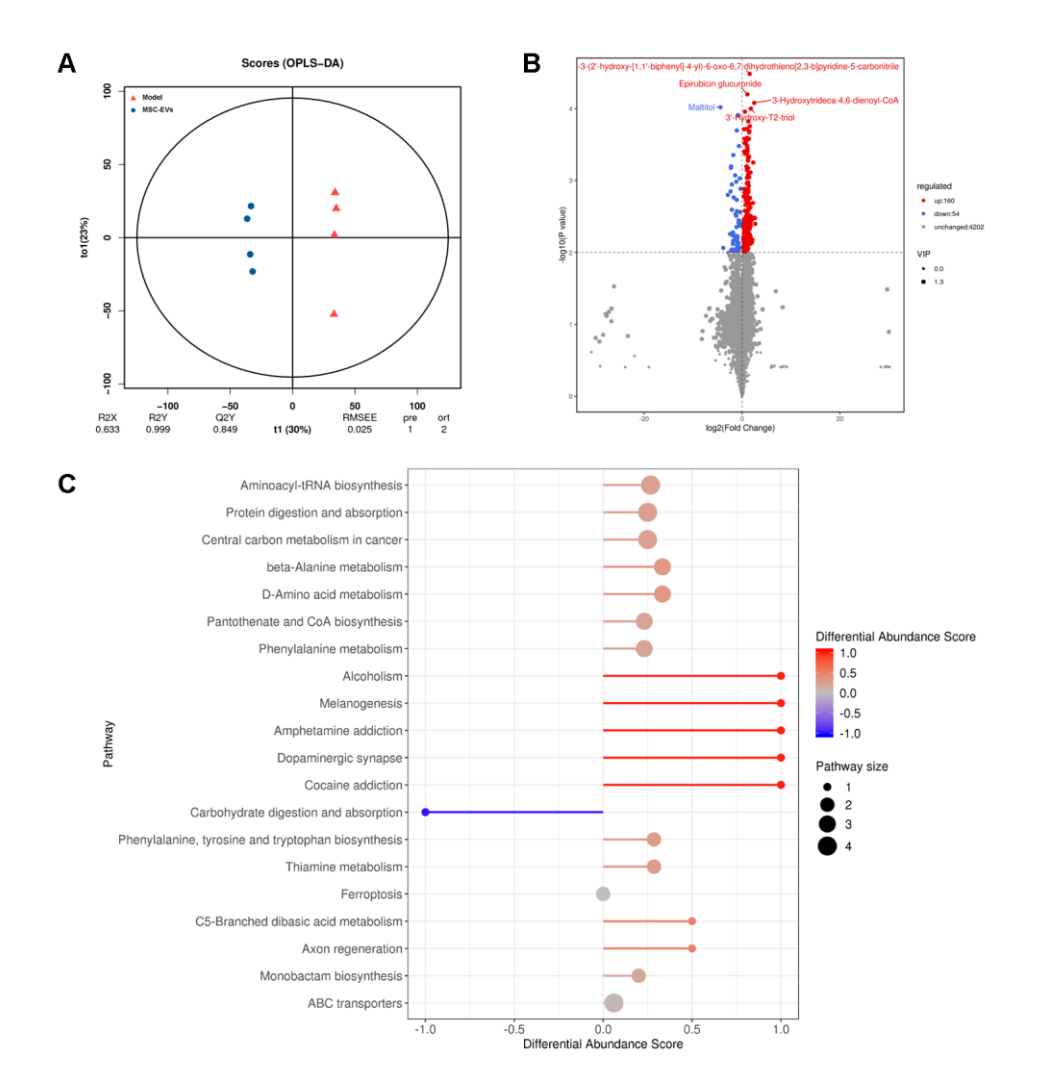
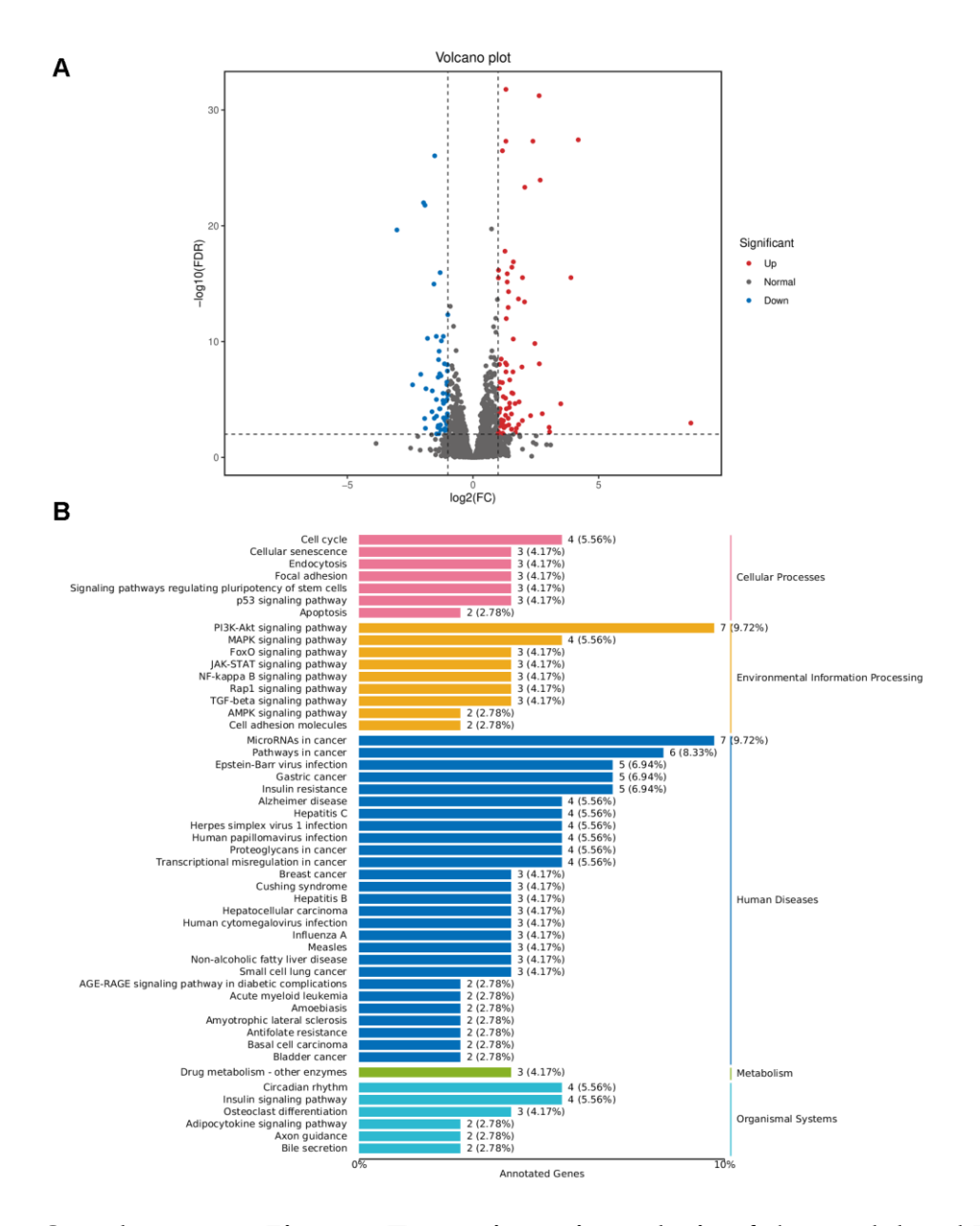
## Supplementary Table 1 The sequences of primers used to conduct quantitative PCR

Gene	Primer	Sequence (5'-3')	Amplicon length (bp)	Organism
P21	Forward	AGGTGGACCTGGAGACCTCAG	139	Human
	Reverse	TCCTCTTGGAGAAGATCAGCCG		
IL-1β	Forward	CGACCAACAAGTGATATTCTC	132	Human
	Reverse	CGACCAACAAGTGATATTCTC		
MMP-1	Forward	TGGACCTGGAGGAAATCTTG	188	Human
	Reverse	GGTACATCAAAGCCCCGATA		
COL-1	Forward	GAGAGCATG ACCGATGGATT	178	Human
	Reverse	CCTTCTTGAGGTTGCCAGTC		
GADPH	Forward	AGGGCTGCTTTTAACTCTGGT	206	Human
	Reverse	CCCCACTTGATTTTGGAGGGA		
18 s	Forward	TAACCCGTTGAACCCCATT	150	Mouse
	Reverse	CCATCCAATCGGTAGTAGCG		
Cu/Zn-SOD	Forward	AACCAGTTGTGTTGTCAGGAC	139	Mouse
	Reverse	CCACCATGTTTCTTAGAGTGAGG		
Mn-SOD	Forward	CAGACCTGCCTTACGACTATGG	113	Mouse
	Reverse	CTCGGTGGCGTTGAGATTGTT		
CAT	Forward	GGAGGCGGAACCCAATAG	102	Mouse
	Reverse	GTGTGCCATCTCGTCAGTGAA		
P21	Forward	ACTACCAGCTGTGGGGTGAG	126	Mouse
	Reverse	TCGGACATCACCAGGATTGG		
IL-1β	Forward	GCCACCTTTTGACAGTGATGAG	95	Mouse
	Reverse	GACAGCCCAGGTCAAAGGTT		



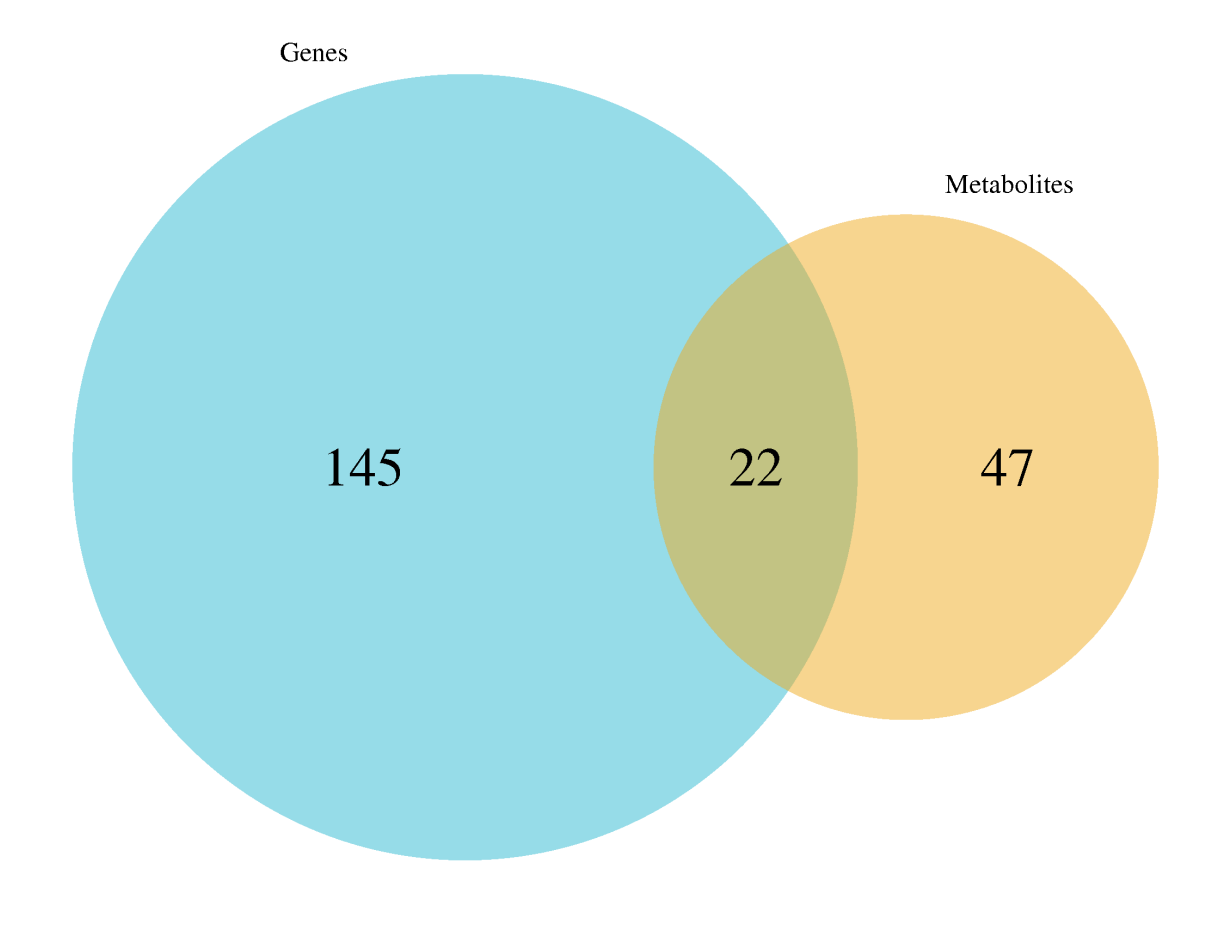
Supplementary Figure 1 Multivariate statistical analysis was performed, and metabolite differences in aging livers after treatment with MSC-EVs were determined. A: An orthogonal partial least squares discriminant analysis score plot was constructed to show the differences between the metabolic profiles of the model and MSC-EV groups; B: A volcano plot of differentially abundant metabolites. A graphical representation highlighting significant changes in metabolite levels between the groups; C: KEGG functional annotation and enrichment analysis of differentially abundant metabolites between the model and MSC-EV groups. The graph depicts the enriched KEGG pathways based on the differential abundance of metabolites and provides insights into the metabolic pathways influenced by MSC-EVs. The metabolites were assigned to KEGG pathways belonging to 13 main

categories, including amino acid metabolism, biosynthesis of other secondary metabolites, cancer overview, carbohydrate metabolism, cell growth and death, digestive system, lipid metabolism, membrane transport, metabolism of cofactors and vitamins, metabolism of other amino acids, nucleotide metabolism, signaling molecules and interactions, and translation.



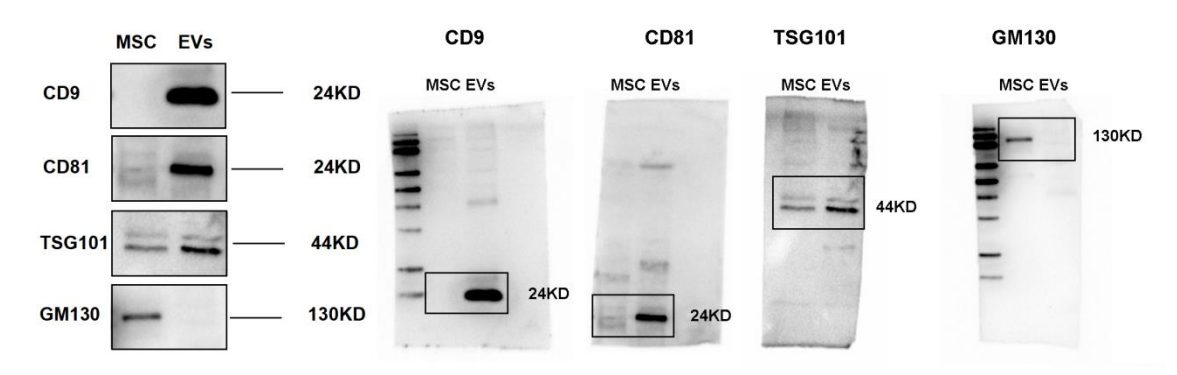
Supplementary Figure 2 Transcriptomic analysis of the model and MSC-EV

**groups.** A: The volcano plot shows differential gene expression between the two groups, with statistical significance against the magnitude of expression change. The volcano plot illustrates the differential expression of genes between two comparative groups. Each point on the plot represents a gene, with the X-axis indicating the fold change in expression (log2 scale) and the Y-axis representing the negative logarithm of the *P* value (-log10 scale); B: KEGG pathway annotation was performed. The differentially expressed genes were categorized according to the KEGG pathways, indicating the potential biological pathways and processes affected.



Model vs EVs-H

Supplementary Figure 3 A Venn diagram of differentially expressed genes and metabolite pathways.



Supplementary Figure 4 Western blot analysis of CD9, CD81, TSG101, and GM130 expression. The protein immunoblotting experiment was designed to detect the expression of CD9, CD81, TSG101, and GM130 in MSCs and their extracellular vesicles. Total protein was extracted using RIPA lysis buffer. The protein concentration was determined by the BCA method. The molecular weight standard was located in the leftmost lane, ranging from 13 kDa to 154 kDa (Servicebio, G2086). CD9 was expected to appear at about 24 kDa. CD81 was expected to appear at about 24 kDa. TSG101 was expected to appear at about 44 kDa. GM130 was expected to appear at about 130 kDa. As shown in the figure, distinct bands corresponding to CD9, CD81, TSG101, and GM130 could be observed in the protein immunoblot.